The effect of changing patient position from supine to prone on the accuracy of a Cosman-Roberts-Wells (CRW) stereotactic head frame system

Torsten Rohlfing[a], Calvin R. Maurer, Jr.[a], David Dean[b], and Robert J. Maciunas[b]

[a]Image Guidance Laboratories, Department of Neurosurgery, Stanford University, Stanford, CA
[b]Department of Neurological Surgery, Case Western Reserve University, Cleveland, OH

ABSTRACT

Despite the growing popularity of frameless image-guided surgery systems, stereotactic head frame systems are widely accepted by neurosurgeons and are still commonly used to perform stereotactic biopsy, functional procedures, and stereotactic radiosurgery. In this study, we investigate the accuracy of the Cosman-Roberts-Wells (CRW) stereotactic frame system when the mechanical load on the frame changes between pre-operative imaging and the intervention due to different patient position—supine during imaging, prone during intervention. We analyze CT images acquired from 12 patients who underwent stereotactic biopsy or stereotactic radiosurgery. Two CT images were acquired for each patient, one with the patient in the supine position and one in the prone position. The prone images were registered to the respective supine images using an intensity-based registration algorithm, once using only the frame and once using only the head. The difference between the transformations produced by these two registrations describes the movement of the patient's head with respect to the frame due to mechanical distortion of the latter. The maximum frame-based registration error between supine and prone positions was 2.8 mm, greater than 2 mm in two patients, and greater than 1.5 mm in five patients. Anterior-posterior translation is the dominant component of the difference transformation for most of these patients. In general, the magnitude of the movement increased with brain volume, which is an index of head weight. We conclude that in order to minimize frame-based registration error due to a change in the mechanical load on the frame, frame-based stereotactic procedures should be performed with the patient in the identical position during imaging and intervention.

Keywords: Stereotactic head frame system, image-guided surgery, intensity-based image registration, target registration error, patient position, mechanical load.

1. INTRODUCTION

Despite the growing popularity of frameless image-guided surgery systems, stereotactic head frame systems are widely accepted by neurosurgeons and are still commonly used to perform stereotactic biopsy, functional procedures, and stereotactic radiosurgery.[1,2] Stereotactic frame systems generally include a stereotactic reference frame (head ring) that provides rigid skull fixation using pins or screws and establishes a stereotactic coordinate system in physical space, a method for stereotactic image acquisition, and a stable mechanical platform (that typically includes an aiming arc assembly) for holding and directing a probe or other surgical instrument to a defined intracranial target point.[2–4] Most current frame systems relate image space to the physical coordinate space established by the reference frame by attaching, just prior to image acquisition, a localizing system consisting of three or more N-shaped fiducials (see Fig. 1).[5,6]

The accuracy of frame-based surgical procedures depends on many things, including image resolution, geometrical fidelity of the images, localization error of the N-shaped fiducials, and the mechanical construction of the frame system. Substantial effort has been made to investigate and quantify some of these sources of error.[7–23] But very

Further author information: (Send correspondence to T.R.)
T.R. and C.R.M.: Image Guidance Laboratories, Department of Neurosurgery, Stanford University, 300 Pasteur Drive, MC 5327, Room S-012, Stanford, CA 94305-5327, phone: +1 (650) 498-7958, fax: +1 (650) 724-4846; T.R.: torsten.rohlfing@stanford.edu; C.R.M.: calvin.maurer@igl.stanford.edu; D.D. and R.J.M.: Department of Neurological Surgery and The Research Institute, University Hospitals of Cleveland, and Department of Neurological Surgery, Case Western Reserve University, 10900 Euclid Avenue, Cleveland, OH 44106-5042, phone: +1 (216) 844-5743, fax: +1 (216) 844-3014; D.D.: daviddean@cwru.edu; R.J.M.: rjm31@po.cwru.edu.

Medical Imaging 2002: Visualization, Image-Guided Procedures, and Display, Seong K. Mun, Editor, Proceedings of SPIE Vol. 4681 (2002) © 2002 SPIE · 1605-7422/02/$15.00

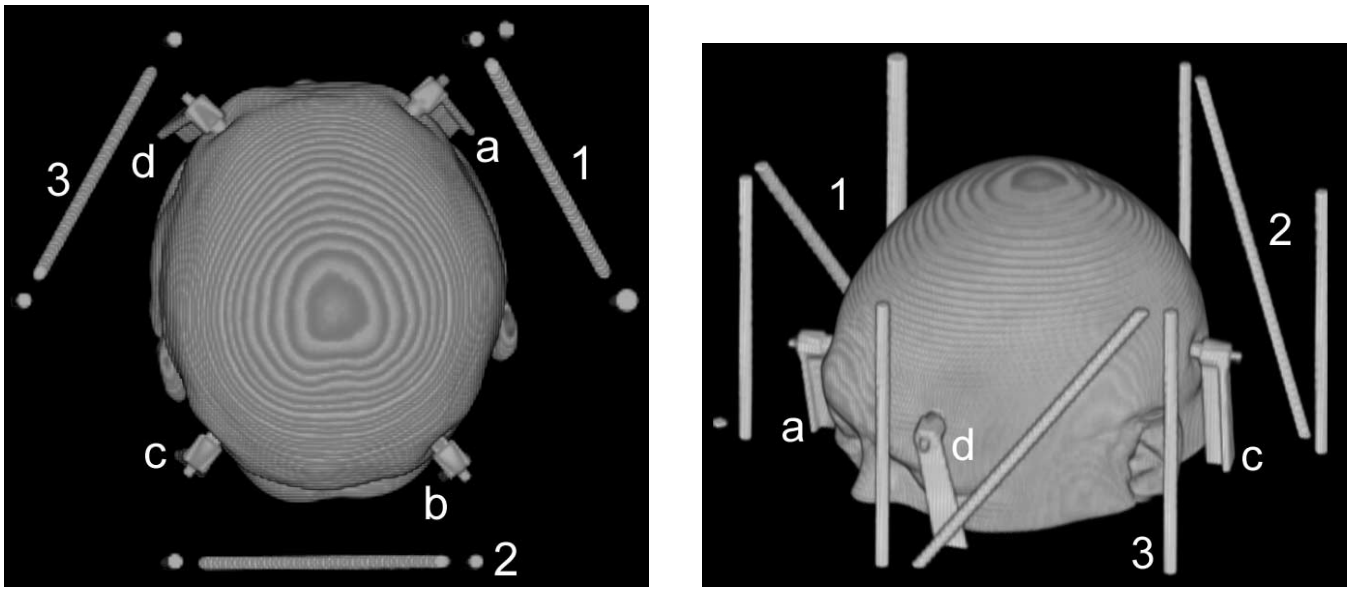

Figure 1. A 3-D volume rendering of a CT image from a patient with an attached stereotactic head frame. *Left:* View from cranial direction, *right:* view from left anterior oblique direction. The stereotactic reference frame or head ring (not visible) is attached to the head by four posts that are labeled "a" through "d". Registration of the image coordinate system to the physical coordinate space established by the reference frame is accomplished by attaching, just prior to image acquisition, a localizing system consisting of three N-shaped fiducials. These fiducials, often referred to as "N-bars", each consists of two parallel and one diagonal rod and are labeled "1" through "3".

little has been reported about the effect of mechanical loading. The accuracy of a frame system depends on its rigidity and the perfect immobilization of the patient's head with respect to the reference frame or head ring, and thus is limited by the construction details of the frame and the mechanical properties of the materials it is manufactured from. Most current stereotactic frame systems attach a reference frame or head ring to the head by four vertical posts using pins or screws. The weight of the head mechanically loads the frame, and the support posts deform. If the mechanical load is identical at the time of scanning and the time of treatment, then the effect is unimportant. If the load is different, the head will move rigidly with respect to the head ring (and the N-shaped fiducials of the localizing system), which defines the stereotactic coordinate system. Even when the patient position is the same at the time of scanning and the time of treatment, there can be a different mechanical load if the body is supported differently in the scanner and the treatment room, as is often the case (the head can generate different force depending on how much the neck and shoulders are supported by the table; also, the head ring support can sit at different vertical heights). The worst case scenario is a supine position during scanning and a prone position during treatment, as is the case, for example, for posterior fossa biopsy and some types of radiosurgery treatment.

The voluntary standard performance specifications for cerebral stereotaxic instruments, as issued by the American Society for Testing and Materials (ASTM), state that the mechanical accuracy of a stereotactic system shall be submillimetric.[24] Nonetheless, two studies using phantoms have reported errors of several millimeters caused by application of mechanical loads similar to the weight of a human head.[15,25] In this study, we use clinical data—CT images acquired from 12 patients who underwent stereotactic biopsy or stereotactic radiosurgery—to investigate the accuracy of a common stereotactic head frame system, the Cosman-Roberts-Wells (CRW) frame system, when the mechanical load on the frame changes due to a change in patient position from supine to prone.

2. METHODS AND MATERIALS

The frame-based registration error due to a change in patient position from supine to prone is equivalent to the movement of the head relative to the N-shaped fiducials caused by the change in mechanical load on the stereotactic frame. We analyze CT images acquired from patients in both the supine and prone positions. Each supine and prone image is segmented into a head-only and a frame-only image. The segmented images are registered to produce

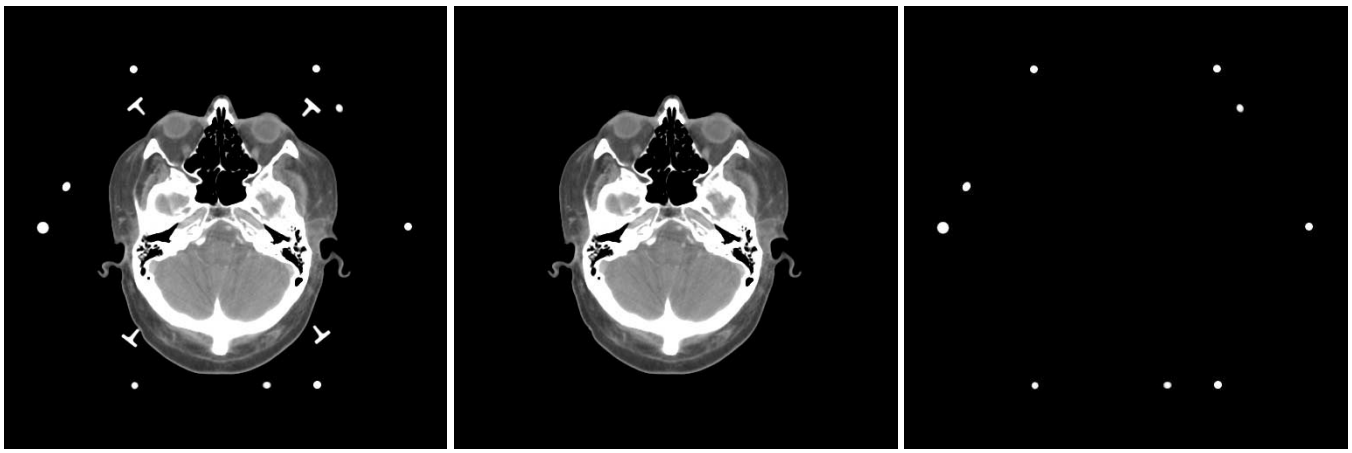

Figure 2. Separation of original CT image (*left*) into head-only (*center*) and frame-only (*right*) images. The three N-bars appear as nine circles (the diagonal rods are ellipses) in a transverse (cross-sectional) image slice such as the one on the left. The four posts used to attach the reference frame (head ring) to the head have a T-shaped cross section in a transverse image. These posts are removed from both the head-only and frame-only images. Thus the frame-only image contains only the three N-bars.

head-only and frame-only supine-to-prone transformations. The difference between these transformations is used to compute the movement of the head relative to the N-shaped fiducials between the supine and prone positions.

2.1. Image acquisition

We analyze CT images acquired from 12 patients who underwent stereotactic biopsy or stereotactic radiosurgery. On the morning of the surgical procedure, a stereotactic reference frame or head ring (Intubation Head Ring, model HRA-IM, Radionics, Burlington, MA) was applied. A localizing system consisting of three N-shaped fiducials (model BRW-LF, Radionics, Burlington, MA) was attached to the stereotactic frame just prior to image acquisition. Two CT images were acquired preoperatively on the morning of the surgical procedure. One image was acquired with the patient in the standard supine position. For this image, the stereotactic frame was mounted to the scanner table via a special adapter. A second image was acquired with the patient in the prone position. Because the frame can mount to the table only in the supine position, for the prone images, the frame was taped to the scanner table and the patient instructed to remain as still as possible during the scan. All images were acquired on a HiSpeed Advantage RP scanner (General Electric Medical Systems, Milwaukee, WI) using conventional table advance. Each image volume contains between 42 and 53 transverse slices with 512×512 pixels. The axial field of view begins just above the frame and ends at the top of the head. The voxel dimensions are typically $0.7 \times 0.7 \times 3.0\,\text{mm}$. All CT image volumes in this study are stacks of image slices with no interslice gap or slice overlap. The gantry tilt angle was zero.

2.2. Image segmentation

Each original CT scan is separated into two distinct images by manual and semi-automatic (region growing) segmentation implemented in a locally developed software package. One of the resulting images contains only the patient's head (head-only image). The other image contains only the three sets of N-shaped fiducials of the localizing system (frame-only image). The segmentation is illustrated in Fig. 2. The intensities of the remaining voxels of the segmented images are set to zero. The four posts used to attach the stereotactic frame (head ring) to the head have a T-shaped cross section in transverse image slices. These posts are removed from both the head-only and frame-only images. This is done because they are the part of the frame system that bears the mechanical load. Deformation of these posts is the cause of movement of the head relative to the stereotactic frame when the patient position changes from supine to prone. Also, image-to-physical registration is accomplished in all current stereotactic frame systems that we are aware of, including in particular the CRW frame system, using only the N-shaped fiducials (e.g., see Refs. 5,6,26,27). We want to compute the frame-based registration error due to a change in patient position from supine to prone, which is equivalent to the movement of the head relative to the N-shaped fiducials caused by the change in mechanical load.

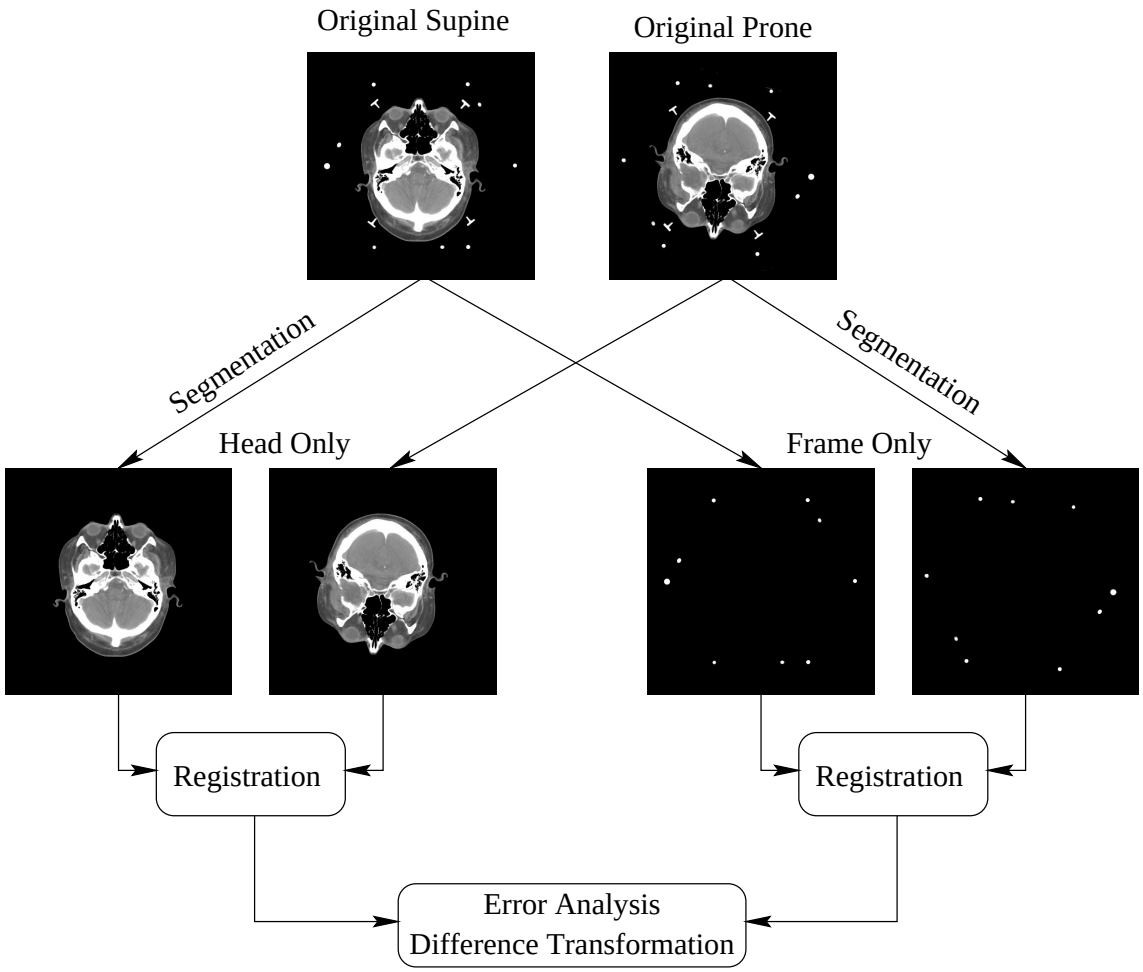

Figure 3. Scheme of image segmentation, registration, and error analysis. The original supine and prone images are separated into head-only (*left branch*) and frame-only (*right branch*) images. The prone head-only image is registered to the supine head-only image. The same is done independently with the prone and supine frame-only images. The resulting transformations are then compared and the error analysis performed as described in the text.

2.3. Image registration

For the head-only and frame-only image data, the images in the supine and prone positions are registered to each other independently. This process is illustrated in Fig. 3. We refer to the registration transformations determined using the head-only and frame-only images as the head-only and frame-only transformations, respectively. Registration is performed using an intensity-based rigid (six degree-of-freedom) registration algorithm. Our technique is based on the normalized mutual information similarity measure.[28] The six parameters of the optimal rigid transformation are determined by a multi-resolution optimization technique. The search algorithm is an independent and modified implementation of the method described in Ref. 29. Our implementation incorporates several additions designed to improve accuracy and computational efficiency of the original algorithm.[30–32] Registration is started with an initial rotation by 180 degrees around the cranial-caudal axis to account for the supine-to-prone relocation of the patient. The registration transformations are visually inspected using subtraction (difference) and fused (interleaved) images (see Figs. 4 and 5).

2.4. Frame-based registration error analysis

We calculate the frame-based registration error due to a change in patient position from supine to prone, which is equivalent to the movement of the head relative to the N-shaped fiducials caused by the change in mechanical load, by using as a reference gold standard the head-only transformation. The head-only transformation was taken as

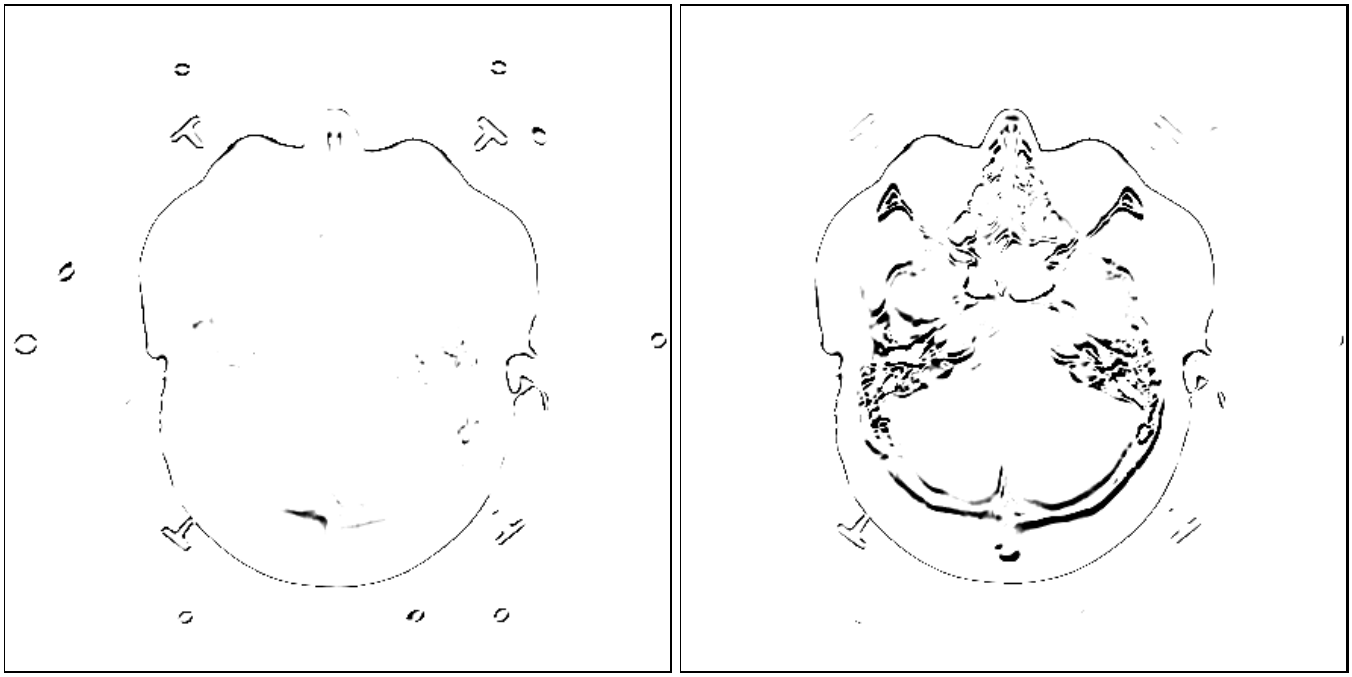

Figure 4. Subtraction (difference) image slices of supine-and-prone study using head-only (*left*) and frame-only (*right*) registration transformations. The lack of artifact inside the head in the head-only registration subtraction image suggests that the head-only registration transformation has subpixel accuracy. The lack of artifact at the N-bar rod cross sections in the frame-only registration subtraction image suggests that the frame-only transformation accurately aligns the N-bars. The artifact inside the head in the frame-only subtraction image indicates that the head moves relative to the N-bars between the supine and prone positions. The artifact at the N-bar rod cross sections in the head-only subtraction image consists primarily of horizontal edges and is consistent with a predominant anterior-posterior translation between the images acquired in the supine and prone positions. Artifacts are present at the skin surface and T-shaped attachment posts in both subtraction images, which suggests that these structures move (and deform) with respect to both the cranium and the N-bars.

the reference because we are interested in accurately registering the patient rather than the frame. Specifically, we calculate the error as the distance between the position of a point in the supine image mapped to the prone image by the reference head-only transformation and its position mapped by the frame-only transformation. The analysis is similar to the one performed in Ref. 33. Let $\mathbf{x}$ be the position of a target point in the supine image. Let $\mathbf{T}_\mathrm{h}$ and $\mathbf{T}_\mathrm{f}$ denote the homogeneous 4×4 matrices representing the head-only and frame-only transformations, respectively. Then $\mathbf{y}_\mathrm{h} = \mathbf{T}_\mathrm{h}\mathbf{x}$ and $\mathbf{y}_\mathrm{f} = \mathbf{T}_\mathrm{f}\mathbf{x}$ are the positions of the target point in the prone image mapped by the head-only and frame-only transformations, respectively. Since $\mathbf{y}_\mathrm{f} = \mathbf{T}_\mathrm{f}\mathbf{x} = \mathbf{T}_\mathrm{f}\mathbf{T}_\mathrm{h}^{-1}\mathbf{y}_\mathrm{h}$, the error is,

$$\Delta\mathbf{y} = \mathbf{y}_\mathrm{f} - \mathbf{y}_\mathrm{h} = (\mathbf{T}_\mathrm{f}\mathbf{T}_\mathrm{h}^{-1} - \mathbf{I})\mathbf{y}_\mathrm{h} \; . \tag{1}$$

We compute the mean, minimum, and maximum values of $\|\Delta\mathbf{y}\|$, i.e., the scalar length of the error vector $\Delta\mathbf{y}$, at all voxels $\mathbf{x}$ inside the patient's brain in the supine study. To achieve this restriction to the interior of the skull, the brains are segmented in the supine images. This is done to ensure that the computed errors represent clinically relevant areas. We also use this segmentation to estimate brain volume, which is an index of head weight. The brain volume values are used to investigate whether there is a relationship between the magnitude of the frame-based error and the (unknown) weight of the head. Since $\mathbf{T}_\mathrm{f}$ and $\mathbf{T}_\mathrm{h}$ are both rigid-body transformations, the difference transformation $\mathbf{T}_\mathrm{f}\mathbf{T}_\mathrm{h}^{-1}$ is also a rigid-body transformation. It can therefore be decomposed into the six common canonical parameters—three translations along the x, y, and z axes, and three successive rotations around these axes. Comparing these parameters to those of the identity transformation (which all have the value zero) provides a more specific description of the nature of the registration error than the mere distribution of differences over the image volume.

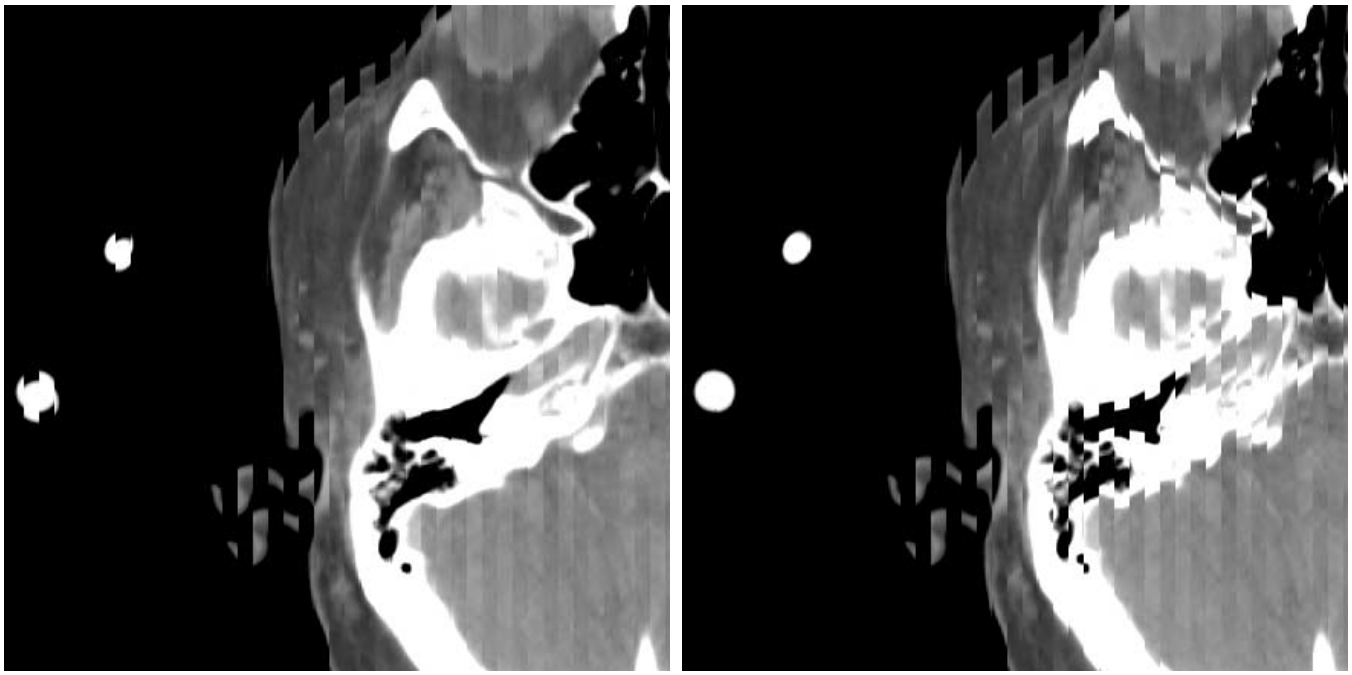

Figure 5. Fused (interleaved) image slices of supine-and-prone study. Alternating vertical bars show corresponding areas of the registered images from both acquisitions. *Left*: Head-only registration, *right*: frame-only registration. This figure shows a zoomed region of the image slice used to generate the subtraction images in Fig. 4. This figure shows, as does Fig. 4, that the head-only registration accurately aligns the cranium and its contents; the frame-only registration accurately aligns the N-bars; the head moves relative to the N-bars between the supine and prone positions; and the skin, temporalis muscle, ears, and eyes deform.

3. RESULTS

The head-only and frame-only registration transformations were visually inspected using subtraction and fused (vertically interleaved) images (see Figs. 4 and 5). The lack of artifact inside the head in the head-only registration subtraction suggests that the head-only registration transformation has subpixel accuracy. The lack of artifact at the N-bar rod cross sections in the frame-only registration subtraction suggests that the frame-only transformation accurately aligns the N-bars. The artifact inside the head in the frame-only subtraction indicates that the head moves relative to the N-bars between the supine and prone positions. The artifact at the N-bar rod cross sections in the head-only subtraction consists primarily of horizontal edges and is consistent with a predominant anterior-posterior translation between the images acquired in the supine and prone positions. Artifacts are present at the skin surface and T-shaped attachment posts in both subtraction images, which suggests that these structures move (and deform) with respect to both the cranium and the N-bars. The subtraction artifacts in Fig. 4 appear as sawtooth artifacts in Fig. 5, which shows fused images in which vertical bars alternate between the registered supine and prone images. Figure 5 shows, as does Fig. 4, that the head-only registration accurately aligns the cranium and its contents; the frame-only registration accurately aligns the N-bars; the head moves relative to the N-bars between the supine and prone positions; and the skin, temporalis muscle, ears, and eyes deform.

The results illustrated in Figs. 4 and 5 are typical of what we observed in 11 of the 12 patients. However, in one patient, we observed substantial misregistration for both the head-only and the frame-only transformations. The apparent cause of the misregistration was substantial patient motion during acquisition of the prone image—visual inspection of the prone image revealed multiple discontinuities in the N-bar rods. This patient was therefore excluded from further analysis.

The results of the quantitative analysis of the frame-based registration error between supine and prone positions are listed for each patient in Table 1. The maximum error was 2.8 mm, was greater than 2 mm in two patients, and was greater than 1.5 mm in five patients. In Fig. 6, the mean and maximum errors for each patient are plotted versus the patient's brain volume, which we use as an index for the (unknown) head weight. There is a slight (the correlation

Table 1. Frame-based registration error between supine and prone positions. Patient 06 was excluded because the patient moved during the prone image acquisition.

Patient	Brain Volume (ml)	Registration Error (mm) min	max	mean
01	1373	0.22	0.44	0.30
02	1582	1.07	1.53	1.27
03	1723	0.68	2.76	1.44
04	1570	0.93	1.18	1.05
05	1110	0.49	1.16	0.75
07	1285	1.11	1.58	1.34
08	1687	0.87	2.03	1.38
09	1094	0.57	0.81	0.69
10	1412	0.42	0.51	0.45
11	1398	0.42	1.52	0.94
12	1492	1.15	1.46	1.30
Mean ± SD	1416 ± 205	0.72 ± 0.32	1.36 ± 0.67	0.99 ± 0.40
Median	1405	0.68	1.46	1.05

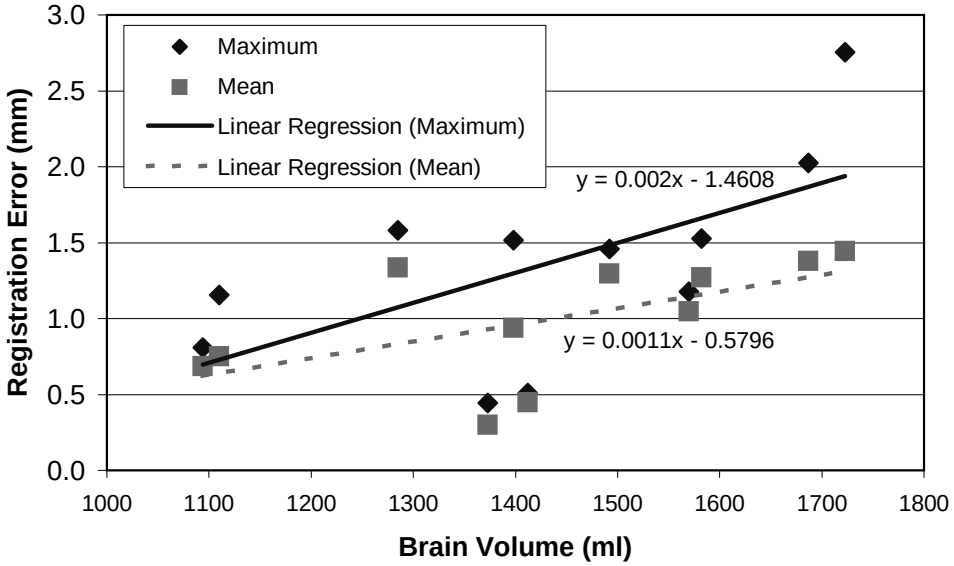

Figure 6. Relationship between frame-based registration error (due to a change in position from supine to prone) and brain volume. The relationship is approximately linear. The correlation coefficients of the mean and maximum error linear regressions are 0.58 and 0.62, respectively. Brain volume is used as an index of head weight.

coefficients of the mean and maximum error linear regressions are 0.58 and 0.62, respectively), but significant ($p < 0.05$), increase in registration error with brain volume.

The difference transformation $\mathbf{T}_\mathrm{f}\mathbf{T}_\mathrm{h}^{-1}$ between the frame-only and head-only registrations was computed and decomposed into the six common canonical parameters—three translations along the x, y, and z axes, and three successive rotations about these axes. Figure 7 is a box-and-whisker plot of the six difference transformation parameters over all patients (see Fig. 8 for the orientation of the image coordinate system relative to the patient). Anterior-posterior translation ("Translation Y" in Fig. 7) is for most of these patients the dominant component of the difference transformation between the frame-only and head-only registrations. This is not unexpected, since it corresponds with the direction of gravity. For one patient, there was a substantial rotation around the x axis, equivalent to a tilting of the head towards the anterior direction. Other translations and rotations showed a somewhat random distribution of relatively minor magnitude.

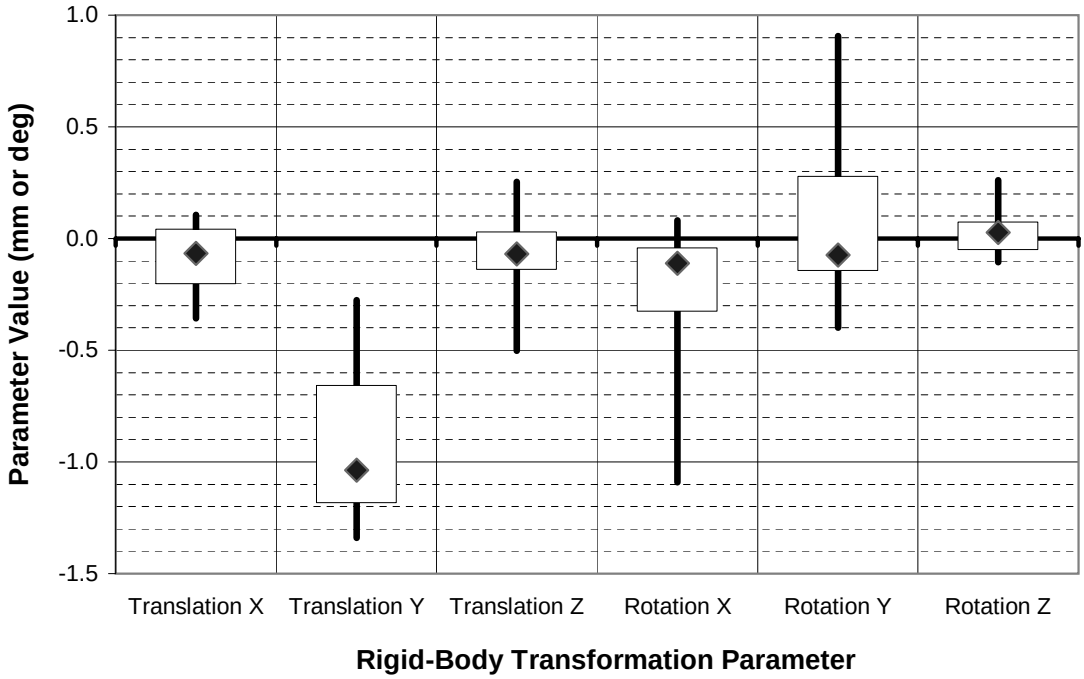

Figure 7. Box-and-whisker plot of the parameters of the difference transformations between frame-only and head-only registrations. The x, y, and z axes are oriented in the right-left, anterior-posterior, and caudal-cranial directions, respectively (see Fig. 8). The diamond denotes the median value of the respective parameter over all patients, the lower and upper edges of the box are the 25^{th} and 75^{th} percentile values, and the ends of the solid line are the minimum and maximum values over all patients. Anterior-posterior translation is for most of these patients the dominant component of the difference transformation between the frame-only and head-only registrations.

4. DISCUSSION

In order to assess the validity of our results, it is necessary to understand how accurately the intensity-based registration algorithm we used registers the frame-only and head-only images. Our registration algorithm was previously validated[30] using the Vanderbilt data sets.[34] The median target registration error for CT-MR registration is approximately 0.6–0.9 mm (the range covers different types of MR images). The head-only and frame-only registrations in this study are serial registrations of monomodality images rather than of multimodal images. An intensity-based registration algorithm, which is similar to the one we used in this study, was found to produce less than 0.2 mm error, which is approximately the threshold of visually detectable change in the difference images, for serial MR registration.[35] The error, which is really registration consistency, was evaluated as the difference between a composition of three transformations forming a cyclic closed loop around three images, $\mathbf{T}_{31}\mathbf{T}_{23}\mathbf{T}_{12}$, and the identity transformation, which is what the composition would produce if there was no registration error in each step. Another intensity-based algorithm, which is also similar to the one we used in this study, was found to achieve 0.4 mm error for registration of pre- and post-operative CT images (unpublished results). The error was evaluated by using as a reference gold standard the point-based registration transformation obtained using five bone-implanted markers.[36] The ability of similar intensity-based registration algorithms to align serial CT and MR images very accurately, and the lack of artifact observed in visual inspection of subtraction images such as those illustrated in Fig. 4, suggest that the head-only and frame-only registration errors are substantially smaller than the amount of measured movement of the head relative to the N-shaped fiducials. Furthermore, the difference transformations between the frame-only and head-only registrations are consistent with what one physically expects—anterior-posterior translation, which corresponds to the direction of gravity, is for most of the patients the dominant component of the difference transformation. The mechanical load, and thus the magnitude of the error, should and does increase with head weight. Finally, errors in the z direction are on the order of magnitude of 0.15 mm and thus are substantially smaller than the resolution of the image data in this direction (slice thickness is 3 mm). This indicates that there were no relevant computational errors induced by between-slice interpolation.

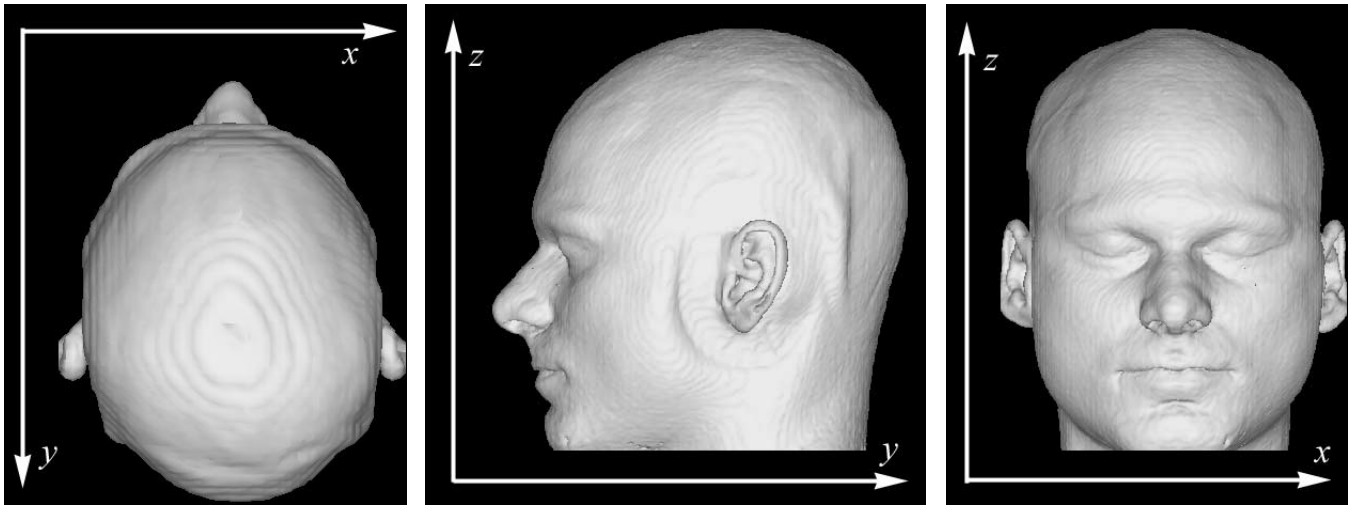

Figure 8. Orientation of the image coordinate system relative to the patient. Axial planes are spanned by the x and y axis, sagittal slices are spanned by y and z, and coronal slices are spanned by x and z.

Thus we believe that the observed effect of changing patient position from supine to prone is real, and that the values of the frame-based registration error between supine and prone that we measured in this study are valid. The error is presumably due to the change in mechanical load that accompanies a change in patient position from supine to prone. The maximum frame-based registration error between supine and prone positions was 2.8 mm, was greater than 2 mm in two patients, and was greater than 1.5 mm in five patients. Errors of this magnitude are sufficiently large enough to potentially cause clinically relevant targeting errors during stereotactic procedures that require submillimetric accuracy. We note that these errors are independent of, and thus potentially in addition to, other sources of error such as image resolution, geometrical fidelity of the images, localization error of the N-shaped fiducials, and the mechanical construction of the frame system.

We conclude that in order to minimize frame-based registration error due a change in the mechanical load on the frame that can accompany a change in patient position, frame-based stereotactic procedures should be performed with the patient in the identical position during imaging and treatment.

5. ACKNOWLEDGMENTS

TR was supported by the National Science Foundation under Grant No. EIA-0104114. TR and CRM acknowledge support for this research provided by CBYON, Inc., Mountain View, CA. DD and RJM acknowledge support from the Research Foundation of the Department of Neurological Surgery, University Hospitals of Cleveland.

REFERENCES

1. E. Alexander, III. and R. J. Maciunas, *Advanced Neurosurgical Navigation*, Thieme Medical Publishers, New York, 1999.
2. P. L. Gildenberg and R. R. Tasker, *Textbook of Stereotactic and Functional Neurosurgery*, McGraw-Hill, New York, 1998.
3. M. P. Heilbrun, ed., *Stereotactic Neurosurgery*, Williams & Wilkins, Baltimore, 1988.
4. P. J. Kelly, *Tumor Stereotaxis*, W. B. Saunders Company, Philadelphia, 1991.
5. R. A. Brown, "A stereotactic head frame for use with CT body scanners," *Invest Radiol* **14**, pp. 300–304, July 1979.
6. R. A. Brown, T. S. Roberts, and A. G. Osborn, "Stereotaxic frame and computer software for CT-directed neurosurgical localization," *Invest Radiol* **15**, pp. 308–312, July 1980.
7. G. Bednarz, M. B. Downes, B. W. Corn, W. J. Curran, and H. W. Goldman, "Evaluation of the spatial accuracy of magnetic resonance imaging-based stereotactic target localization for gamma knife radiosurgery of functional disorders," *Neurosurgery* **45**, pp. 1156–1163, 1999.

8. R. Bhagwandien, *Object Induced Geometry and Intensity Distortions in Magnetic Resonance Imaging*. PhD thesis, Utrecht University, Utrecht, The Netherlands, 1994.
9. D. Dean, J. Kamath, J. L. Duerk, and E. Ganz, "Validation of object-induced MR distorsion correction for frameless stereotactic neurosurgery," *IEEE Trans Med Imaging* **17**, pp. 810–816, Oct. 1998.
10. S. Dong, J. M. Fitzpatrick, and R. J. Maciunas, "Rectification of distortion in MRI for stereotaxy," in *Proc. Fifth Annual IEEE Symposium on Computer-Based Medical Systems*, pp. 181–189, IEEE Computer Society Press, Los Alamitos, CA, 1992.
11. J. M. Fitzpatrick, C. R. Maurer, Jr., and J. J. McCrory, "Phantom testing of ACUSTAR I with comparison to stereotaxy," Tech. Rep. CS-94-04, Department of Computer Science, Vanderbilt University, June 1994.
12. P. A. Hardy and G. H. Barnett, "Spatial distortion in magnetic resonance imaging: Impact on stereotactic localization," in *Textbook of Stereotactic and Functional Neurosurgery*, P. L. Gildenberg and R. R. Tasker, eds., pp. 271–280, McGraw-Hill, New York, 1998.
13. D. L. G. Hill, C. R. Maurer, C. Studholme, J. M. Fitzpatrick, and D. J. Hawkes, "Correcting scaling errors in tomographic images using a nine degree of freedom registration algorithm," *J Comput Assist Tomogr* **22**(2), pp. 317–323, 1998.
14. R. J. Maciunas, J. M. Fitzpatrick, S. Gadamsetty, and C. R. Maurer, Jr., "A universal method for geometric correction of magnetic resonance images for stereotactic neurosurgery," *Stereotact Funct Neurosurg* **66**, pp. 137–140, 1996.
15. R. J. Maciunas, R. L. Galloway, Jr., and J. W. Latimer, "The application accuracy of stereotactic frame," *Neurosurgery* **35**, pp. 682–694, Oct. 1994.
16. C. R. Maurer, Jr., G. B. Aboutanos, B. M. Dawant, S. Gadamsetty, R. A. Margolin, R. J. Maciunas, and J. M. Fitzpatrick, "Effect of geometrical distortion correction in MR on image registration accuracy," *J Comput Assist Tomogr* **20**(4), pp. 666–679, 1996.
17. R. A. Meuli, F. R. Verdun, F. O. Bochud, L. Emsley, and H. Fankhauser, "Assessment of MR image deformation for stereotactic neurosurgery using a tagging sequence," *Am J Neuroradiol* **15**, pp. 45–49, 1994.
18. J. Michiels, H. Bosmans, P. Pelgrims, D. Vandermeulen, J. Bybels, G. Marchal, and P. Suetens, "On the problem of geometric distortion in magnetic resonance images for stereotactic neurosurgery," *Magn Reson Imaging* **12**, pp. 749–765, 1994.
19. L. R. Schad, H.-H. Ehricke, B. Wowra, G. Layer, R. Engenhart, H.-U. Kauczor, H.-J. Zabel, G. Brix, and W. J. Lorenz, "Correction of spatial distortion in magnetic resonance angiography for radiosurgical treatment planning of cerebral arteriovenous malformations," *Magn Reson Imaging* **10**, pp. 609–621, 1992.
20. T. S. Sumanaweera, J. R. Adler, S. Napel, and G. H. Glover, "Characterization of spatial distortion in MRI and its implications for stereotactic surgery," *J Neurosurg* **35**, pp. 696–704, 1994.
21. T. S. Sumanaweera, G. H. Glover, P. F. Hemler, P. A. Van den Elsen, D. Martin, J. R. Adler, and S. Napel, "MR geometric distortion correction for improved frame-based stereotaxic target localization accuracy," *Magn Reson Med* **34**, pp. 106–113, 1995.
22. D. J. Wyper, J. W. Turner, J. Patterson, B. R. Condon, K. W. M. Grossart, A. Jenkins, and D. M. Hadley, "Accuracy of stereotaxic localisation using MRI and CT," *J Neurol Neurosurg Psychiatry* **49**, pp. 1445–1448, 1986.
23. C. Yu, M. L. J. Apuzzo, C.-S. Zee, and Z. Petrovich, "A phantom study of the geometric accuracy of computed tomographic and magnetic resonance imaging stereotactic localization with the Leksell stereotactic system," *Neurosurgery* **48**, pp. 1092–1098, May 2001.
24. American Society for Testing and Materials Committee F-4.05, "Standard performance specification for cerebral stereotactic instruments," in *Annual Book of ASTM Standards, F 1266-89*, pp. 1–6, American Society for Testing and Materials, Philadelphia, 1990.
25. M. C. Schell, A. Perec, D. Rosenzweig, C. R. Maurer, Jr., A. B. Soni, T. Barry, A. Matloubieh, and G. Beranek, "Tumor position displacement as a function of patient orientation for stereotactic frames." Oral presentation at the World Congress on Medical Physics and Biomedical Engineering, Chicago, IL, Jul 23-28, 2000.
26. M. P. Heilbrun, S. Koehler, P. MacDonald, V. Siemionow, and W. Peters, "Preliminary experience using an optimized three-point transformation algorithm for spatial registration of coordinate systems: A method of noninvasive localization using frame-based stereotactic guidance systems," *J Neurosurg* **81**, pp. 676–682, 1994.
27. B. A. Kall, P. J. Kelly, and S. J. Goerss, "Interactive stereotactic surgical system for the removal of intracranial tumors utilizing the CO_2 laser and CT-derived database," *IEEE Trans Biomed Eng* **32**, pp. 112–116, 1985.

28. C. Studholme, D. L. G. Hill, and D. J. Hawkes, "An overlap invariant entropy measure of 3D medical image alignment," *Pattern Recognit* **33**(1), pp. 71–86, 1999.
29. C. Studholme, D. L. G. Hill, and D. J. Hawkes, "Automated three-dimensional registration of magnetic resonance and positron emission tomography brain images by multiresolution optimization of voxel similarity measures," *Med Phys* **24**, pp. 25–35, Jan. 1997.
30. T. Rohlfing, *Multimodale Datenfusion für die bildgesteuerte Neurochirurgie und Strahlentherapie*. PhD thesis, Technische Universität Berlin, 2000.
31. T. Rohlfing, "Efficient voxel lookup in non-uniformly spaced images using virtual uniform axes," in *Medical Imaging: Image Processing*, M. Sonka and K. M. Hanson, eds., vol. 4322 of *Proceedings of SPIE*, pp. 986–994, Feb. 2001.
32. T. Rohlfing and J. Beier, "Improving reliability and performance of voxel-based registration by coincidence thresholding and volume clipping," in *Proceedings of Medical Image Understanding and Analysis*, D. J. Hawkes, D. L. G. Hill, and R. Gaston, eds., pp. 165–168, King's College, (London, UK), July 1999.
33. C. R. Maurer, Jr., R. J. Maciunas, and J. M. Fitzpatrick, "Registration of head CT images to physical space using a weighted combination of points and surfaces," *IEEE Trans Med Imaging* **17**, pp. 753–761, Oct. 1998.
34. J. B. West, J. M. Fitzpatrick, M. Y. Wang, B. M. Dawant, C. R. Maurer, Jr., R. M. Kessler, R. J. Maciunas, C. Barillot, D. Lemoine, A. Collignon, F. Maes, P. Suetens, D. Vandermeulen, P. A. van den Elsen, S. Napel, T. S. Sumanaweera, B. Harkness, P. F. Hemler, D. L. G. Hill, D. J. Hawkes, C. Studholme, J. B. A. Maintz, M. A. Viergever, G. Malandain, X. Pennec, M. E. Noz, G. Q. Maguire, Jr., M. Pollack, C. A. Pelizzari, R. A. Robb, D. Hanson, and R. P. Woods, "Comparison and evaluation of retrospective intermodality brain image registration techniques," *J Comput Assist Tomogr* **21**(4), pp. 554–566, 1997.
35. M. Holden, D. L. G. Hill, E. R. E. Denton, J. M. Jarosz, T. C. S. Cox, T. Rohlfing, J. Goodey, and D. J. Hawkes, "Voxel similarity measures for 3D serial MR brain image registration," *IEEE Trans Med Imaging* **19**, pp. 94–102, Feb. 2000.
36. C. R. Maurer, Jr., J. M. Fitzpatrick, M. Y. Wang, R. L. Galloway, Jr., R. J. Maciunas, and G. S. Allen, "Registration of head volume images using implantable fiducial markers," *IEEE Trans Med Imaging* **16**, pp. 447–462, Aug. 1997.